HHS Public Access

Author manuscript

Radiat Res. Author manuscript; available in PMC 2024 April 01.

Published in final edited form as:

Radiat Res. 2023 April 01; 199(4): 319–335. doi:10.1667/RADE-22-00178.1.

A C57L/J Mouse Model of the Delayed Effects of Acute Radiation Exposure in the Context of Evolving Multi-Organ Dysfunction and Failure after Total-Body Irradiation with 2.5% Bone Marrow Sparing

Allison Gibbs[a,1], **Pawan Gupta**[b], **Buddha Mali**[a], **Yannick Poirier**[a], **Mathangi Gopalakrishnan**[b], **Diana Newman**[a], **Andrew Zodda**[a], **Julian D. Down**[c], **Artur A. Serebrenik**[d], **Michael D. Kaytor**[d], **Isabel L. Jackson**[e]

[a]Division of Translational Radiation Sciences, Department of Radiation Oncology, University of Maryland School of Medicine, Baltimore, Maryland 21201

[b]Center for Translational Medicine, University of Maryland School of Pharmacy, Baltimore, Maryland 21201

[c]Massachusetts Institute of Technology, Cambridge, Massachusetts 02139

[d]Humanetics Corporation, Minneapolis, Minnesota 55435

[e]True North BioPharm, LLC, Rockville, Maryland 20854

Abstract

Gibbs A, Gupta P, Mali B, Poirier Y, Gopalakrishnan M, Newman D, Zodda A, Down JD, Serebrenik AA, Kaytor MD, Jackson IL, A C57L/J Mouse Model of the Delayed Effects of Acute Radiation Exposure in the Context of Evolving Multi-Organ Dysfunction and Failure after Total-Body Irradiation with 2.5% Bone Marrow Sparing. Radiat Res. 199, 319–335 (2023).

The objective of the current study was to establish a mouse model of acute radiation syndrome (ARS) after total-body irradiation with 2.5% bone marrow sparing (TBI/BM2.5) that progressed to the delayed effects of acute radiation exposure, specifically pneumonitis and/or pulmonary fibrosis (DEARE-lung), in animals surviving longer than 60 days. Two hundred age and sex matched C57L/J mice were assigned to one of six arms to receive a dose of 9.5 to 13.25 Gy of 320 kV X-ray TBI/BM2.5. A sham-irradiated cohort was included as an age- and sex-matched control. Blood was sampled from the facial vein prior to irradiation and on days 5, 10, 15, 20, 25, and 30 postirradiation for hematology. Respiratory function was monitored at regular intervals throughout the in-life phase. Animals with respiratory dysfunction were administered a single 12-day tapered regimen of dexamethasone, allometrically scaled from a similar regimen in the non-human primate. All animals were monitored daily for up to 224 days postirradiation for signs of organ dysfunction and morbidity/mortality. At euthanasia due to criteria or at the study endpoint, wet lung weights were recorded, and blood sampled for hematology and serum

[1] Corresponding author: Allison Gibbs, B.S., Program Director, Laboratory Research, Division of Translational Radiation Sciences, Department of Radiation Oncology, University of Maryland School of Medicine, Medical School Teaching Facility, Room 760, 685 West Baltimore Street, Baltimore, Maryland 21201; AGibbs@som.umaryland.edu.

chemistry. The left lung, heart, spleen, small and large intestine, and kidneys were processed for histopathology. A dose-response curve with the estimated lethal dose for 10–99% of animals with 95% confidence intervals was established. The median survival time was significantly prolonged in males as compared to females across the 10.25 to 12.5 Gy dose range. Animal sex played a significant role in overall survival, with males 50% less likely to expire prior to the study endpoint compared to females. All animals developed pancytopenia within the first one- to two-weeks after TBI/BM2.5 followed by a progressive recovery through day 30. Fourteen percent of animals expired during the first 30-days postirradiation due to ARS (e.g., myelosuppression, gastrointestinal tissue abnormalities), with most deaths occurring prior to day 15. Microscopic findings show the presence of radiation pneumonitis as early as day 57. At time points later than day 70, pneumonitis was consistently present in the lungs of mice and the severity was comparable across radiation dose arms. Pulmonary fibrosis was first noted at day 64 but was not consistently present and stable in severity until after day 70. Fibrosis was comparable across radiation dose arms. In conclusion, this study established a multiple organ injury mouse model that progresses through the ARS phase to DEARE-lung, characterized by respiratory dysfunction, and microscopic abnormalities consistent with radiation pneumonitis/fibrosis. The model provides a platform for future development of medical countermeasures for approval and licensure by the U.S. Food and Drug Administration under the animal rule regulatory pathway.

INTRODUCTION

Nonclinical development of medical countermeasures (MCM) for mitigation and/or treatment of life-threatening illness after acute exposure to ionizing radiation at doses of 2 Gy or above requires animal models that mirror the clinical disease in humans (1). The signs and symptoms of acute radiation syndrome (ARS) manifest within the first days to weeks after exposure to high doses of radiation to all or most of the body (2). Individuals who survive the ARS are at risk for developing the delayed effects of acute radiation exposure (DEARE) over the weeks to months that follow. ARS and DEARE are characterized by a constellation of syndromes associated with multiorgan dysfunction and failure (3). The clinical syndromes reflect not only the radiosensitivity of the progenitor and stem cell compartments (e.g., bone marrow, gastrointestinal tract, lung), but also the pathobiological complexity of the disease (e.g., endotheliopathy, coagulopathy, inflammation, fibrosis) (4, 5).

MCMs for ARS and/or DEARE are developed for approval and licensure under the U.S. Food and Drug Administration (FDA) Animal Rule, a non-traditional regulatory pathway that relies on demonstrated therapeutic efficacy in well-powered, well-controlled studies conducted in one or more well-characterized animal models as a surrogate for clinical trials in humans (6). In addition to efficacy, a robust safety profile, known mechanism of action targeting key biological pathways underlying disease development, and adequate assurances of therapeutic dosing in humans based on the drug pharmacodynamic (PD)/pharmacokinetic (PK) profile are prerequisites for MCM approval. To date, four MCMs have been approved for label expansion under the Animal Rule based on demonstrated efficacy in mouse and non-human primate models of total-body irradiation (TBI) for the treatment of myelosuppression associated with ARS based on the ability to accelerate recovery

from neutropenia (i.e., filgrastim, peg-filgrastim, sargramostim) and thrombocytopenia (i.e., romiplostim) leading to an improvement in overall survival (7–12). As animal models serve as a surrogate due to ethical and feasibility considerations, the bar for efficacy is purposely set high to provide reasonable assurance that the results will translate to improved outcomes in humans. The validity of animal models relies on their ability to recapitulate the signs and symptoms of the disease in humans, reflect the underlying biological mechanism of disease progression, and predict clinical outcomes in humans (13).

The mouse (and to a lesser extent the rat) has been extensively used in preclinical research to model TBI-induced ARS and organ-specific sequelae after localized irradiation to inform on the biological mechanisms of disease and perform early MCM efficacy screens to elucidate the best dose, route, and schedule of administration. The mouse is an ideal species for modeling normal tissue response to radiation due to a deep literature database with well-characterized molecular, cellular, and immune responses, genetic diversity including in-bred and outbred strains, and availability of genetically modified animals (1, 14, 15).

The objective of the current study was to develop a C57L/J mouse model of DEARE, specifically radiation pneumonitis and pulmonary fibrosis (DEARE-lung), in the context of evolving multiorgan injury associated with ARS after TBI with 2.5% bone marrow sparing (TBI/BM2.5). The C57L/J mouse strain was selected as lung injury is well characterized in this model after whole thorax lung irradiation (WTLI) and after TBI with bone marrow transplant (BMT), and the phenotype of radiation-induced lung injury in this strain mirrors the anticipated disease in humans (15–18).

WTLI and TBI with “top off” doses have been traditionally used to evaluate MCM efficacy against DEARE-lung in other mouse strains of higher radiation resistance (19). However, current studies were designed based on expected outcome in humans and feedback received from the FDA during a pre-investigational new drug meeting regarding the drug development plan for BIO 300 (Humanetics Corporation, Minneapolis, MN) as a MCM for DEARE-lung. Given the likelihood of hematologic acute radiation syndrome (H-ARS) developing together with gastrointestinal (GI) ARS among individuals exposed to supratherapeutic radiation doses in a nuclear disaster, and the subsequent development of late normal tissue responses in individuals surviving through ARS, the FDA recommended an animal model that will assess the efficacy of BIO 300 within the setting of multiorgan injury and failure rather than localized exposures (20). To this end, hematology parameters, body weight, respiratory function and other signs of disease onset, progression, and resolution or failure were monitored during the in-life phase to establish the profile of disease progression. Serum chemistry, gross exam, organ weights, and post-mortem microscopic exam of vital tissues at necropsy provided a comprehensive overview of the disease pathology for comparison with the reported pathogenesis in the NHP and human. The result was the development of a product-independent animal model platform for MCM development including pharmacokinetics/pharmacodynamics, dose-schedule optimization, and pivotal efficacy studies to bring new and repurposed pharmacological interventions to approval under the FDA Animal Rule regulatory pathway.

MATERIALS AND METHODS

Animals

Two hundred age and sex matched C57L/J mice (females: 17.0–22.7 g, males: 24.1–32.6 g, The Jackson Laboratory, Bar Harbor, ME), aged 10–12 weeks on the day of irradiation, were included on this study. Animals were housed, five per cage, in microisolater cages containing certified direct contact bedding [Harlan Teklad (Envigo, Frederick, MD) soft cob bedding, 1/4'' corn cob with enrichment]. Room temperatures were maintained at 23 ± 3°C (68–79°F) with 30 to 70% relative humidity. A 12-hour light/dark cycle was maintained by Veterinary Resources. Due to the potential incidence of incisor abnormalities and loss when the head is in the radiation field (21, 22), animals were provided DietGel® Recovery (Clear H2O, Westbrook, ME) ad libitum in addition to the standard food [2018 Teklad Global 18% Protein diet (Envigo, Frederick, MD)] and chlorinated water (7–9 ppm) in a Hydropact®, manufactured by the University of Maryland, Baltimore, throughout the study.

Identification, Allocation and Randomization

Animals were identified by a unique tag applied to the pinna of the mouse ear by research staff no earlier than 48 h after on-site receipt from the vendor. If during the study the ear tag was damaged or inadvertently removed, the animal was re-tagged, and all prior ear tag numbers were recorded for traceability. Animals were randomly assigned to radiation dose arms based on cage number.

Total-Body Irradiation with 2.5% Bone Marrow Sparing

Unanesthetized animals were restrained in a hexagonal jig and exposed to a single uniform total-body irradiation from a 320 kV Orthovoltage X-ray radiation source (320 kVp, HVL = 1 mm Cu, dose rate 1.662 ± 0.03 Gy/min, X-Rad 320, Precision X-ray, North Branford, CT) with lead shielding of the tibiae (2.5% BM) (FIg. 1). The hexagonal jig remains stationary during animal irradiation. The radiation doses were 9.5, 10.25, 11, 11.75, 12.5 and 13.25 Gy (n = 15 males and 15 females per dose). Sham-irradiated controls (n = 10 males and 9 females) were treated in the same way except the source was not turned on. Radiation exposure (including sham irradiation) is performed between 9 am and 1 pm to reduce chronoradiosensitivity as a biological variable (23). Two animals were excluded prior to study initiation due to not meeting the criteria for inclusion. Therefore, exceptions to the final enrollment numbers were 9 females in the sham arm (i.e., n = 19 total) and 14 males in the 10.25 Gy arm (i.e., 29 total).

The X-ray irradiator absolute dose was calibrated in accordance with the American Association of Physicists in Medicine TG-61 protocol with a National Institutes of Standards and Technology (NIST)-traceable Farmer type ionization chamber: TN30013, SN 009805 (PTW, Freiburg, Germany) and electrometer: UNIDOS E TN10010, SN 001106 (PTW, Freiburg, Germany) calibrated biannually by K & S Associates, Inc. (Nashville, TN) to ensure accuracy in dose delivery. The absorbed dose rate under animal irradiation conditions was measured in a mouse-mimicking polystyrene phantom using a pinpoint ionization chamber: CC04, SN 11324 (IBS Dosimetry, Bartlett, TN) that was cross-calibrated with NIST-traceable Farmer chamber. Measurements were performed in all 6

possible positions to ensure animals receive the same dose (within ±0.5%) at each position. The TG61 calibration was verified annually by a recognized third-party dosimetry service (Radiation Dosimetry Services, MD Anderson, Houston, TX). The radiation exposure times were calculated using the dose rate measured in the mouse mimicking phantom. Prior to any animal irradiation, output measurements were performed daily using a cross-calibrated ion chamber corrected for daily pressure and temperature.

Frequency and Schedule of Observations

Animals were observed in their home cage once per day, at a minimum, seven days per week to monitor signs of morbidity and mortality. Animals were observed for posture, gait, coat, activity, malocclusions, behavior, and dermatitis. Animal body weight was collected pre-irradiation and, at a minimum, every 5 ± 2 days postirradiation (e.g., 10% or greater body weight loss or other indications of distress are observed). Rodent incisors were evaluated at least once per week during the clinical exam throughout the in-life phase of the study due to tooth loss after irradiation when the head is in-field.

Blood Sampling and Hematology

Blood samples were collected from the facial vein prior to irradiation (between days −14 and −5) and on days 5, 10, 15, 20, 25 and 30 after TBI/BM2.5 or sham irradiation, where day 0 = irradiation day. Blood was also collected from the inferior vena cava at the time of scheduled or unscheduled euthanasia immediately following administration sodium pentobarbital (100 mg/kg, IP) for hematology. Samples were analyzed for complete blood count by automated analysis using a Beckman Coulter Ac.T diff™ (Beckman Coulter, Inc., Miami, FL) followed by a 5-part manual differential and evaluation of cellular abnormalities on peripheral blood smears.

Respiratory Function

Respiratory function was assessed during the in-life phase using unrestrained, non-invasive whole-body plethysmograph (WBP, Buxco Research System, Wilmington, NC). Pulmonary function was assessed at baseline (pre-irradiation) and weeks 2, 4, 6, 8, and 10. After week 10, pulmonary function was assessed twice per week until the pre-determined study endpoint (220 days). Briefly, mice were allowed to acclimate in a barometric chamber for at least 5 minutes, and the recording of the breathing pattern was performed for 10 min. Every 30 s during the recording session, respiratory rate (bpm), tidal volume (mL), minute volume (mL/min), enhanced pause (Penh, index of constriction), pause (index of constriction), Rpef (ratio of Te->PEF: Total Te), compliance (unitless), estimated peak inspiratory flow (mL/s), estimated peak expiratory flow (mL/s), inspiratory time (s), expiratory time (s), expiratory flow at 50% expired volume (mL/s), end inspiratory pause (ms), end expiratory pause (ms), and relaxation time (Tr), was determined by the Buxco software (Buxco Research System, Wilmington, NC).

Dexamethasone

Same sex animals were administered dexamethasone in a tapered regimen when animals of the same sex within a radiation group exhibited a mean twofold increase in Penh. Penh was

recorded twice per week during the period when animals were at risk of pulmonary injury (i.e., days 70 through 220). Animals who relapsed were not treated with any additional dexamethasone. The regimen was allometrically scaled from the non-human primate (24). Briefly, animals were treated with dexamethasone at a dose of 5.8 mg/kg (IP) twice per day on day 1, 2.9 mg/kg (IP) twice per day on days 2–4, 2.9 mg/kg (IP) once per day on days 5–7, and 2.9 mg/kg (IP) every other day on days 8, 10, and 12, relative to the day of treatment initiation (i.e., day 1).

Euthanasia Criteria and Necropsy

To determine if the condition of a moribund animal qualifies it for euthanasia, the animal was evaluated using the criteria summarized as follows: a single criteria of anorexia (≥30% body weight loss between day 1–45; >20% body weight loss between day 46 and 220) -or- moribund and exhibiting no movement even when stimulated; or a combination criterion of at least three of the four following criteria met on the same day: 1. >25% body weight loss (between days 0 and 45), >15% body weight loss (between days 46 and 220), 2. inactivity, defined as no movement unless actively stimulated, 3. lack of grooming that worsens after 24 h, 4. abnormal appearance, e.g., persistent hunched posture, piloerection, and/or hypothermia (i.e., cold to the touch). The body weight criteria for the ARS versus the DEARE-phase were established based on differences in the manifestation of illness phase where weight loss occurs due to gastrointestinal damage within the first two-weeks postirradiation and full recovery has been empirically observed at up to 25–28% loss.

Animals designated for necropsy (either by criteria above, or by having survived to the planned end of the study) were euthanized by sodium pentobarbital (100 mg/kg, IP). After blood collection from the inferior vena cava, a bilateral thoracotomy was performed. Detailed gross necropsies were performed and consisted of a complete external and internal examination.

Pleural fluid was measured, if observed, and the lungs and heart were removed. Lungs were separated (left vs. right); weights were individually collected and recorded. The three right lung lobes were separated and snap frozen in liquid nitrogen for tissue cytokine analysis or hydroxyproline measurements. The heart weight was collected and recorded. The left lung lobe (inflated ex vivo through the bronchi with 10% neutral buffered formalin), heart, spleen, and gastrointestinal tract (e.g., jejunum, duodenum, ileum, and colon), and kidneys were fixed in 10% neutral buffered formalin for histopathology.

Histopathology

Tissues were shipped in formalin to Histo-Scientific Research Laboratories (HSRL, Inc., Mt. Jackson, VA), a StageBio Company, for histology and pathology evaluation and reporting. Slides were evaluated by a board-certified veterinary pathologist. Fibrosis was scored using a modified fibrosis scoring system (MFSS) based on the Ashcroft scale with a range of 0–8 (25). For example, Grade 0 fibrosis was defined as no fibrotic burden of the alveolar septa and normal lung structure. Grade 3 fibrosis was defined as contiguous fibrotic walls of the alveolar septa (i.e., septum >3× thicker than normal) predominantly in the whole microscopic field and partly enlarged alveoli and rarefied, but no fibrotic masses. Grade 5

was defined as severely damaged, but still preserved lung structure with confluent fibrotic masses (10–50% of the microscopic field). Grade 8 fibrosis was defined as non-existent alveolar septa with complete fibrotic obliteration of the lung structure.

Data Analysis

The proportion of animals that survived for 220 days and the median survival times (length of time corresponding to a survival probability of 50%) were computed for each of the radiation dose groups and by sex. Kaplan-Meier plots were used to visualize survival curves for the different radiation dose groups overall and by sex. The radiation dose-response curve was estimated by performing a probit regression on the binary response variable (survival) as a function of the logarithm of the radiation dose.

The standard error for the $LD_{xx/220}$ estimate was determined by the delta method and was used to obtain the asymptotic 95% confidence intervals. The mean (±SE) plots were used to explore the differences in the longitudinal trends of respiratory, hematological parameters between the different irradiation groups. All analyses and were performed using R version 4.0.2 (2020–06-22) (R Foundation for Statistical Computing, Vienna, Austria) running under the RStudio interface (Free Software Foundation, Inc., Boston, MA).

RESULTS

Overall Survival after TBI/BM2.5 in 10–12 Week of Age Male and Female C57L/J Mice

Early mortality was observed in the first 30-days postirradiation, with most events occurring in the first 15-days postirradiation. None of the animals in the sham-irradiated cohort expired during the first 30 days. The highest mortality during the ARS phase was observed in the 11–13.25 Gy arms with 13% mortality in the 11 Gy arm, 20% in the 11.75 Gy arm, 13% in the 12.5 Gy arm, and 23% in the 13.25 Gy arm. Bone marrow failure and gastrointestinal abnormalities consistent with ARS were common findings.

The onset of major morbidity/mortality associated with DEARE was inversely correlated to radiation dose and occurred between days 59 to 164 after TBI/BM2.5. The latency period for male C57L/J mice was longer than that observed in female mice across all radiation arms, except 13.25 Gy, as shown by the median survival time (Table 1). Kaplan-Meier curves for 220-day survival for male and female C57L/J mice exposed to 9.5 to 13.25 Gy of TBI/BM2.5 with 320 kV X rays are shown in Fig. 2A and B, respectively.

Based on the temporal incidence of DEARE-lung and the plateau in major morbidity/mortality beyond study day 180, probit-estimated lethality was determined at 180-day for the purposes of dose selection for future studies. Probit curves for 180-day survival with 95% confidence interval for male and female mice are shown in Fig. 2C and 2D. The Probit-estimated lethal dose for 10–99% of animals within 180-days after TBI/BM2.5 is shown in Table 2. Probit-estimated lethality profiles were also generated for 150-day and 220-day survival (Supplementary [2] Fig. S1A and B; https://doi.org/10.1667/RADE-22-00178.1.S1).

[2]Editor's note. The online version of this article (DOI: https://doi.org/10.1667/RADE-22-00178.1) contains supplementary information that is available to all authorized users.

Significant Difference in Overall Survival between Male and Female C57L/J mice after TBI/BM2.5 at Doses between 9.5 to 13.25 Gy

The difference in survival between male and female C57L/J mice was statistically significant. The dose modifying factor (DMF) for male C57L/J mice with respect to female C57L/J mice on 220-day survival was 1.05. The DMF for male sex on both 150- and 180-day survival was 1.04. Based on cox-proportional hazards regression analysis, the hazard ratio for 220-day survival in male mice compared to female mice was 0.51 (95% confidence interval (CI): 0.37, 0.70). This suggests there was a significant difference in 220-day survival between male and female mice ($P < 0.0001$), i.e., the hazard of death for male C57L/J mice was approximately 50% lower than female mice. Further, the analysis showed that, for a given sex of the animal, the hazard of death is increased two-fold (hazard ratio – 1.96; 95% CI: 1.70, 2.25) for each incremental increase (i.e., 75 cGy) in radiation dose.

Pancytopenia Associated with ARS during the First 30-Days after TBI/BM2.5

Animals developed pancytopenia associated acute radiation sickness during the first 30-days postirradiation. Longitudinal changes in the absolute lymphocyte count (ALC) (Fig. 3A), absolute neutrophil count (ANC) (Fig. 3B), platelet count (Fig. 3C), red blood cell count (Fig. 3D), and hemoglobin (Fig. 3E) show a similar declining trend in the mean (±SE) between baseline (pre-irradiation) and day 5 for ANC or day 10 for platelet count, hemoglobin, and red blood cell counts. Hematology parameters began to recovery between days 15–20. The longitudinal mean of cell counts (e.g., neutrophils, platelets, and red blood cells) and hemoglobin over the first 30-days after TBI/BM2.5 were found to be similar among animals expiring prior to the study endpoint and 220-day survivors. The duration of neutropenia and recovery of ANC to >1,000 cell/μl was consistently longer in female mice than male mice (Table 3). The mean time to first day for platelet cell counts less than 50,000 and 20,000 cells/ul was 10 days. Only 6 animals had platelet count less than 20,000 cells/μl. The duration of thrombocytopenia and recovery of platelets to >50,000 cell/μl was observed to be similar between males and females. However, the frequency of blood draws (i.e., every 5 days between day 0 and 30) may have masked differences due to the rapid rate of decline and recovery of hematology parameters. Mean platelet nadir was slightly lower in female mice as compared to male mice. The 13.25 Gy group demonstrated slightly slower, stable and less drop in longitudinal mean hemoglobin levels compared to other radiation groups.

Functional Manifestation of Lung Injury Associated with DEARE in C57L/J mice after TBI/BM2.5

Female C57L/J met the protocol-defined criteria for initiation of dexamethasone starting on weeks 11 (12.5 Gy) or 12 (11, 11.75 or 13.25 Gy), 13 (10.25 Gy) or 15 (9.5 Gy) after TBI/BM2.5 (Supplemental Fig. S2; https://doi.org/10.1667/RADE-22-00178.1.S1). In contrast, male C57L/J mice in the 9.5 Gy arm did not trigger for dexamethasone treatment (i.e., the mean Penh did not double in this group) during the 220-day follow-up after TBI/BM2.5. Male C57L/J mice exposed to 10.25 or 13.25 Gy triggered in week 13, those exposed to 11 or 11.75 Gy triggered in week 14, and animals exposed to 12.5 Gy triggered in week 12 after TBI/BM2.5. None of the sham-irradiated controls triggered for treatment with dexamethasone.

Longitudinal changes in pulmonary function after TBI/BM2.5 in C57L/J mice is shown in Fig. 4. The latency period prior to the onset in respiratory dysfunction is approximately 10 weeks. A marked increase in Penh (unitless measurement of airway congestion, Fig. 4A) was observed coincident with the increased incidence of mortality between 70–180 days (10 – ~26 weeks) after TBI/BM2.5. A decrease in Penh was observed concomitant with the initiation of dexamethasone treatment; however, the response was not durable beyond the completion of treatment. An immediate rebound in Penh followed by rapid onset of mortality was observed (Supplemental Fig. 2; https://doi.org/10.1667/RADE-22-00178.1.S1). Changes in end expiratory pause (EEP, Fig. 4B), inspiratory time (Ti, Fig. 4C), and expiratory time (Te, Fig. 4D) were also noted.

Edema/Congestion and Histological Evidence of Radiation Pneumonitis/Fibrosis

Wet lung weights, an indicator of edema/congestion are shown in Fig. 5A–D by sex and survival outcome. Left and right wet lung weights were significantly higher in male C57L/J mice exposed to 9.5–12.5 Gy, but not 13.25 Gy when compared to the sham-irradiated control arm ($P < 0.1$ vs. control, Fig. 5A and B, Table 4). The left wet lung weight in female C57L/J mice exposed to 10.25 and 11 Gy was significantly higher than the sham-irradiated controls ($P = 0.0004$ and $P = 0.0015$ vs. controls, respectively, Fig. 5C, Table 4). Data also revealed that female mice exposed to 9.5 Gy, 10.25 Gy, and 11 Gy had significantly higher right wet lung weights compared to the sham-irradiated controls ($P < 0.01$, Fig. 5D, Table 4). Pleural effusions were not observed.

Representative micrographs of tissue abnormalities and architectural distortion after radiation are shown in Fig. 5E–J. Microscopic findings consistent with radiation pneumonitis (including hyaline membranes, interstitial inflammation with necrosis and fibrin thrombi, infiltration of alveolar spaces by macrophages and perivascular mononuclear infiltrates) were not consistently observed until later time points. One animal showed pathological findings consistent with pneumonitis/fibrosis as early as study day 57. At time points later than study day 70, pneumonitis was consistently present and comparable between irradiated groups. Significant fibrosis in association with pneumonitis was noted at study day 64 in a single animal but was more consistently present at later time points. Mild to moderate fibrosis was consistently present at time points later than study day 70 in all treatment groups.

There was a significant increase in lung fibrosis among irradiated animals. The incidence of moderate fibrosis was particularly marked among animals surviving to the study endpoint (Fig. 6).

Other Pathological Manifestations of Acute and Delayed Radiation Injury after TBI/BM2.5 in C57L/J Mice

Figure 7A and B shows the blood urea nitrogen (BUN) at euthanasia for the different radiation groups by sex and survival outcome. No clear trend is seen in the BUN distribution among animals expiring prior to the study endpoint. Elevated BUN (>30 mg/dL) at the time of euthanasia was observed in ten animals. Nine of the 10 incidences occurred in the first

120-days postirradiation. BUN > 30 mg/dL was observed in only a single animal surviving to the study endpoint.

Figure 7C and D depicts lactate levels at euthanasia for the different radiation groups by sex and survival outcome. Lactate levels were markedly elevated among animals surviving to the study endpoint in male mice in the 10.25 Gy arm.

Figure 7E and F show heart weights among animals euthanized prior to the study endpoint or at the time of scheduled euthanasia. There was a significant decrease in heart weights among C57L/J mice expiring prior to the study endpoint as compared to the sham controls. By 220 days, the heart weights were not significantly different between irradiated animals and the sham-control. Statistical comparisons for BUN, lactate levels, and heart weights are shown in Table 5.

Figure 7G–I shows representative micrographs of radiation-associated microscopic findings in the spleen and intestines. Degeneration and apoptosis of intestinal crypt epithelium with crypt hyperplasia and villus blunting, lymphoid depletion in the spleen and increased extramedullary hematopoiesis (EMH) in the spleen were observed. Changes in the intestinal tract and lymphoid depletion were primarily observed at very early time points (≤day 16). Microscopic findings of the gastrointestinal tract and spleen of eight animals exposed to 11.0 and 13.25 Gy and expiring between days 6 and 16 showed mild to moderate apoptosis of crypt epithelium, minimal crypt abscesses, mild to moderate crypt hyperplasia, mixed cell inflammation, marked to severe lymphoid depletion, and markedly to severely increased EMH. Moderate to severe villus blunting and mixed cell inflammation of the gastrointestinal tract/mucosa were observed, but not consistently. An increase in EMH was also observed at later time points. Additional microscopic findings that were considered unrelated to irradiation (due to the sporadic occurrence, presence in control group, and/ or are common background findings in mice) included mononuclear infiltrates in the heart and kidneys (data not shown).

DISCUSSION

The objective of the current study was to develop a mouse model of radiation pneumonitis/ fibrosis in the context of evolving multiorgan injury associated with TBI across a dose-range expected to induce ARS progressing to DEARE-lung. Furthermore, it is anticipated that this model would be used for the development of MCMs to be submitted for approval under the FDA Animal Rule regulatory pathway.

The model was designed to provide a product-independent platform for testing the safety, PK/PD, and efficacy of MCMs for the mitigation of ARS/DEARE. The study design involved extensive discussion and concurrence with the study sponsor, Humanetics Corporation, the Radiation and Nuclear Countermeasures Program at the National Institutes of Allergy and Infectious Diseases, and the FDA, Division of Imaging and Radiation Medicine.

To accomplish the objectives of this study, age- and sex-matched C57L/J mice (10–12 weeks of age) were selected as the appropriate species/strain based on prior literature (15,

26, 27). There is a rich diversity in phenotypic outcomes among mouse and rat strains following localized lung irradiation that have been extensively characterized and exploited to identify the genetic determinants of disease (28–31). The C57L/J strain was previously characterized as developing an early pneumonitis and late fibrosis phenotype mirroring the response observed in both the non-human primate and the human lung. Further, the ability to dissociate pneumonitis from fibrosis through pharmacological intervention and radiation dose fractionation suggests these pathologies are not inextricably linked (15, 32). Therefore, separate MCMs will likely be required to effectively target the pathophysiological mechanisms underlying the two disease conditions and demonstrate a therapeutic benefit against life-threatening acute pneumonitis and chronic, debilitating fibrosis.

The left tibia of each animal was shielded in this study to avoid dose-limiting hematopoietic failure and assess the evolution of ARS to DEARE over a 220-day period postirradiation. In a radiological or nuclear incident, it is anticipated that individuals will be exposed to inhomogeneous doses of irradiation and therefore this model more closely resembles the human situation (20). The precise percentage of bone marrow spared due to shielding of the left tibia is unclear as formal studies of regional active hematopoiesis were not performed. However, it is estimated based on the literature that the model spares approximately 2 to 2.5% of the bone marrow (33).

In this study, the Probit-predicted lethal dose for 50% of animals, by sex, within the first 180-days after TBI/BM2.5 was estimated as 10.01 Gy in male C57L/J mice and 9.66 Gy in female C57L/J mice. The $LD_{70/180}$ is estimated as 10.29 Gy and 9.86 Gy, in male and female C57L/J mice, respectively. Data demonstrated female mice were significantly more radiosensitive than males after TBI/BM2.5. The dose modifying effect of sex on 220, 180, and 150-day survival was 1.05, 1.04 and 1.04, respectively. This is similar to the Chinese-bred rhesus macaque where the lethal dose for 50% of animals within the first 180-days ($LD_{50/180}$) after whole thorax lung irradiation is estimated as 10.24 Gy (95% CI: 9.87–10.52 Gy) for male and 10.28 Gy (95% CI: 9.68–10.92) for female animals (34). In those studies, no significant difference in the $LD_{50/180}$ between male vs. female non-human primates was observed. In partial-body exposures with 5% bone marrow sparing, the $LD_{50/180}$ was 9.95 Gy (95% CI: 9.35–10.29), demonstrating the similarity in pulmonary radiation dose response between the C57L/J mouse strain and the non-human primate. Likewise, the onset of clinical pneumonitis in humans after a single dose of whole lung irradiation is approximately 7.5 Gy with 100% incidence occurring after doses of 11–12 Gy (35).

Similar to the non-human primate model of partial body irradiation with bone marrow sparing, the $LD_{50/180}$ was lower in both male and female C57L/J mice after TBI/BM2.5 compared to whole thorax lung irradiation (34). This is likely, in part, a result of 30-day mortality due to ARS and evolving multiorgan injury associated with DEARE. In a C57L/J mouse model of TBI with bone marrow transplant (BMT), animals developed severe, lethal radiation pneumonitis approximately 4 months postirradiation with focal fibrotic lesions observed in animals surviving to the 8-month study endpoint (17). The pathobiological phenotype of lung injury in the TBI/BM2.5 model was closely similar to that observed in

the C57L/J model of TBI plus BMT. The TBI/BM2.5 model is considered more suitable for evaluation of MCM efficacy to mitigate and/or treat DEARE-lung as BMT is not generally recommended for radiation injuries.

The clinical course of ARS progressing to DEARE has been documented in rat and non-human primate models as well as humans. To monitor the onset, severity, and duration of myelosuppression associated with ARS in animals exposed to TBI/BM2.5, blood was sampled at scheduled time points prior to irradiation and from days 5–30 postirradiation. Acute renal toxicity was evaluated based on reported results in the rat model of TBI with bone marrow shielding demonstrating significant renal impairment associated with the DEARE (36, 37). Although renal injury has been reported to arise later in mice than in rats, a renal panel, including blood urea nitrogen, was performed in serum samples collected at the time of euthanasia due to cause or upon reaching the study endpoint. Respiratory function was monitored at baseline and throughout the in-life phase. At the time of unscheduled or scheduled euthanasia, a gross exam of vital organs was performed, and organ weights collected. Post-mortem microscopic exam of tissues was performed to evaluate the pathology of multiorgan injury.

Animals developed myelosuppression associated with acute radiation sickness during the first 30 days. Approximately 25 animals (11.9%) expired during the ARS phase. Among animals euthanized due to criteria for major morbidity during the ARS phase, microscopic findings included degeneration and apoptosis of intestinal crypt epithelium with crypt hyperplasia and villus blunting, lymphoid depletion in the spleen consistent with the clinical pathology of ARS. Changes in the intestinal tract and lymphoid depletion were primarily observed at very early time points (≤day16). Increased extramedullary hematopoiesis in the spleen was present primarily at later time points.

The primary endpoint for survival was 180-days based on prior data. However, the in-life phase was extended to 220-days postirradiation to monitor the progression of disease until major morbidity/mortality reached a sustained plateau. The rationale was based on guidance from the FDA to inform upon the length of future studies to adequately monitor the durability of MCM response. The majority of deaths due to DEARE occurred between study days 70 and 150 after which mortality reached a plateau.

Animals were treated with dexamethasone when the mean Penh, a unitless measure of airway congestion that corresponds to acute respiratory distress, doubled for an individual treatment cohort (i.e., segregated by radiation dose and animal sex). Dexamethasone was administered to animals on a population-based trigger to treat schedule and at a dose allometrically scaled from the non-human primate to the mouse due to minimal existing literature to provide appropriate dosing information. In this study, male C57L/J mice in the 9.5 Gy arm did not reach the necessary threshold for respiratory dysfunction to require treatment with dexamethasone; whereas female mice exposed to 9.5 Gy arm triggered for treatment during week 15 after TBI/BM2.5. Both male and female mice exposed to 10.25 Gy TBI/BM2.5 triggered during week 13. In animals exposed to 11 or 11.75 Gy, female mice triggered for treatment during week 12 compared to week 14 in male mice. At 12.5 or 13.25 Gy, female C57L/J mice met criteria for dexamethasone treatment in weeks 11 or

12, respectively, compared to weeks 12 or 13, respectively, in male mice. In all groups, Penh decreased in response to dexamethasone treatment, but the response was not durable once treatment stopped.

The delayed onset of respiratory distress, measured by Penh, in male C57L/J mice was consistent with the reduced rate of mortality compared to female C57L/J mice. In the 9.5 Gy arm, 180-day mortality was 20% in male C57L/J mice compared to 33.3% in female C57L/J mice. At 10.25 Gy, mortality was 57.1% versus 93.3% in male versus female mice, respectively. However, at doses of 11 Gy or higher, there was 100% mortality in both sexes by day 180 after TBI/BM2.5. The effect of dexamethasone on study outcomes cannot be fully elucidated as non-treated comparator arms were not included. However, at a minimum, treatment with dexamethasone did not appear to improve overall survival on day 180.

In the 13.25 Gy arm, particularly among male mice, death appeared to be primarily due to damage to organs other than the lung (e.g., decreased heart weight, limited edema/congestion as determined by lung weight). It is likely that this is the threshold dose for injury to one or more organs that manifest earlier than the lung.

The supportive care regimen utilized in this study was carefully considered. In mutual agreement with the study sponsor, the model was developed in the absence of the current standard of care (e.g., antibiotics, cytokine therapy) to minimize animal stress resulting from multiple procedures (e.g., daily subcutaneous injections to administer cytokine therapy). However, it is expected that MCM development will include a superiority/non-inferiority study with cytokine therapy (e.g., Neupogen®, Neulasta® or Leukine®) during early efficacy screening to define the best dose and schedule have been completed.

Antibiotics were not included to harmonize the model with existing TBI models in the mouse at other national institutions. A review of the literature suggests administration of enrofloxacin, a first-line antibiotic in large animal models of ARS, in the drinking water is not recommended due to the pharmacokinetics of the drug (38, 39). It was determined that therapeutic plasma concentrations could not be achieved except through daily subcutaneous injections. Further, Plett et al. found no significant 30-day survival advantage for animals treated with ciprofloxacin and levofloxacin when compared to the no-antibiotic support arm (23). Efficacy data in those studies did demonstrate a benefit with neomycin-treated water and doxycycline chow. However, as swollen muzzle syndrome is not an outcome observed at the University of Maryland School of Medicine (UMSOM) in mouse models exposed to total or partial body irradiation, it was determined that the benefit did not outweigh the risk (e.g., antibiotic resistance, etc.).

The TBI/BM2.5 model allows development of ARS, but with hematological recovery among the majority of animals. Animals surviving through the ARS phase progress to multiorgan dysfunction and failure, including DEARE-lung. The natural history of disease progression following TBI/BM2.5 is consistent with both experimental data generated in the non-human primate model of TBI with 5% bone marrow sparing and anecdotal evidence in humans where victims survived through the ARS phase with moderate to advanced supportive care measures only to then go on to develop life-threatening radiation pneumonitis/fibrosis. In

parallel to the current study, a 180-day study was conducted in the non-human primate model of TBI/BM5 at a dose (10.0 Gy) resulting in 75% mortality among the vehicle control arm in the presence of advanced supportive care (e.g., cytokine therapy, blood transfusions, and steroids). Comparative analysis between the models will be the subject of future studies to bridge potential knowledge gaps in the natural history of disease progression and therapeutic efficacy of medical countermeasure interventions. Taken together, the model appears to be adequate for screening medical countermeasures for DEARE-lung in the context of evolving multiorgan injury associated with TBI/BM2.5.

In summary, the C57L/J mouse model of TBI/BM2.5 in the dose range of 9.5–13.25 Gy progresses through the acute radiation syndrome to go on to develop delayed effects of acute radiation exposure, namely pneumonitis and fibrosis. This model recapitulates the pathogenesis observed in non-human primates after total-body irradiation with 5% bone marrow sparing and in humans based on anecdotal evidence from radiation accidents (40).

Supplementary Material

Refer to Web version on PubMed Central for supplementary material.

ACKNOWLEDGMENTS

We thank Lanyn Taliaferro, Ph.D., who kindly reviewed the manuscript. This study was supported by a subcontract under the National Institutes of Allergy and Infectious Disease (NIAID)/National Institutes of Health (NIH) Contract Number HHSN272201800011C awarded to Humanetics Corporation, subcontract to the University of Maryland School of Medicine and by a NIAID/NIH Center for Medical Countermeasures against Radiation awarded to the University of Maryland School of Medicine (U19 AI150574).

REFERENCES

1. Williams JP, Jackson IL, Shah JR, Czarniecki CW, Maidment BW, DiCarlo AL, Animal models and medical countermeasures development for radiation-induced lung damage: report from an NIAID Workshop. Radiat Res 2012; 177, e0025–e39. [PubMed: 22468702]
2. Wolbarst AB, Wiley AL Jr., Nemhauser JB, Christensen DM, Hendee WR, Medical response to a major radiologic emergency: a primer for medical and public health practitioners. Radiology 2010; 254, 660–77. [PubMed: 20177084]
3. Williams JP, McBride WH, After the bomb drops: a new look at radiation-induced multiple organ dysfunction syndrome (MODS). Int J Radiat Biol 2011; 87, 851–68. [PubMed: 21417595]
4. Bentzen SM, Preventing or reducing late side effects of radiation therapy: radiobiology meets molecular pathology. Nat Rev Cancer 2006; 6, 702–13. [PubMed: 16929324]
5. Fajardo LF, The pathology of ionizing radiation as defined by morphologic patterns. Acta Oncol 2005; 44, 13–22. [PubMed: 15848902]
6. FDA, Guidance for industry: product development under the animal rule. US Food and Drug Administration 2015; 21 CFR 314.600–650 for drugs; 21 CFR 601.90–95 for biologics, Docket Number: FDA-2009-D-0007.
7. Farese AM, Bennett AW, Gibbs AM, Hankey KG, Prado K, Jackson W 3rd, et al. , Efficacy of Neulasta or Neupogen on H-ARS and GI-ARS Mortality and Hematopoietic Recovery in Nonhuman Primates After 10-Gy Irradiation With 2.5% Bone Marrow Sparing. Health Physics 2019; 116, 339–53. [PubMed: 30281533]
8. Farese AM, Cohen MV, Katz BP, Smith CP, Gibbs A, Cohen DM, et al. , Filgrastim improves survival in lethally irradiated nonhuman primates. Radiat Res 2013; 179, 89–100. [PubMed: 23210705]

9. Wong K, Chang PY, Fielden M, Downey AM, Bunin D, Bakke J, et al. , Pharmacodynamics of romiplostim alone and in combination with pegfilgrastim on acute radiation-induced thrombocytopenia and neutropenia in non-human primates. Int J Radiat Biol 2020; 96, 155–66. [PubMed: 31216213]
10. Bunin DI, Bakke J, Green CE, Javitz HS, Fielden M, Chang PY, Romiplostim (Nplate((R))) as an effective radiation countermeasure to improve survival and platelet recovery in mice. Int J Radiat Biol 2020; 96, 145–54. [PubMed: 31021662]
11. Zhong Y, Pouliot M, Downey AM, Mockbee C, Roychowdhury D, Wierzbicki W, et al. , Efficacy of delayed administration of sargramostim up to 120 hours post exposure in a nonhuman primate total body radiation model. Int J Radiat Biol 2021; 97, S100–S16. [PubMed: 32960660]
12. Hankey KG, Farese AM, Blaauw EC, Gibbs AM, Smith CP, Katz BP, et al. , Pegfilgrastim Improves Survival of Lethally Irradiated Nonhuman Primates. Radiat Res 2015; 183, 643–55. [PubMed: 26035709]
13. Denayer T, Stohr T, Roy MV, Animal models in translational medicine: Validation and prediction. European Journal of Molecular & Clinical Medicine 2014; 2, 5–11.
14. Boerma M, Davis CM, Jackson IL, Schaue D, Williams JP, All for one, though not one for all: team players in normal tissue radiobiology. Int J Radiat Biol 2022; 98, 346–66. [PubMed: 34129427]
15. Dabjan MB, Buck CM, Jackson IL, Vujaskovic Z, Marples B, Down JD, A survey of changing trends in modelling radiation lung injury in mice: bringing out the good, the bad, and the uncertain. Lab Invest 2016; 96, 936–49. [PubMed: 27479087]
16. Jackson IL, Xu PT, Nguyen G, Down JD, Johnson CS, Katz BP, et al. , Characterization of the dose response relationship for lung injury following acute radiation exposure in three well-established murine strains: developing an interspecies bridge to link animal models with human lung. Health Physics 2014; 106, 48–55. [PubMed: 24276549]
17. Down JD, Yanch JC, Identifying the high radiosensitivity of the lungs of C57L mice in a model of total-body irradiation and bone marrow transplantation. Radiat Res 2010; 174, 258–63. [PubMed: 20681792]
18. Jackson IL, Xu P, Hadley C, Katz BP, McGurk R, Down JD, et al. , A preclinical rodent model of radiation-induced lung injury for medical countermeasure screening in accordance with the FDA animal rule. Health Physics 2012; 103, 463–73. [PubMed: 22929472]
19. Cassatt DR, Gorovets A, Karimi-Shah B, Roberts R, Price PW, Satyamitra MM, et al. , A Trans-Agency Workshop on the Pathophysiology of Radiation-Induced Lung Injury. Radiat Res 2022; 197, 415–33. [PubMed: 34342637]
20. Satyamitra MM, Cassatt DR, Marzella L, A Trans-Agency Workshop on the Pathophysiology of Radiation-Induced Lung Injury. Radiat Res 2022; 197, 408–14. [PubMed: 34714907]
21. Down JD, Tarbell NJ, Warhol M, Mauch P, Dose-limiting complications from upper half body irradiation in C3H mice. International Journal of Radiation Oncology, Biology, Physics 1988; 14, 483–9. [PubMed: 3277932]
22. Pearson AE, Phelps TA, Radiation effects on mouse incisor teeth following whole-body doses of up to 16 gray. Int J Radiat Biol Relat Stud Phys Chem Med 1981; 39, 409–17. [PubMed: 6971849]
23. Plett PA, Sampson CH, Chua HL, Joshi M, Booth C, Gough A, et al. , Establishing a murine model of the hematopoietic syndrome of the acute radiation syndrome. Health Physics 2012; 103, 343–55. [PubMed: 22929467]
24. Garofalo M, Bennett A, Farese AM, Harper J, Ward A, Taylor-Howell C, et al. , The delayed pulmonary syndrome following acute high-dose irradiation: a rhesus macaque model. Health Physics 2014; 106, 56–72. [PubMed: 24276550]
25. Hubner RH, Gitter W, El Mokhtari NE, Mathiak M, Both M, Bolte H, et al. , Standardized quantification of pulmonary fibrosis in histological samples. Biotechniques 2008; 44, 507–11, 14–7. [PubMed: 18476815]
26. Jackson IL, Vujaskovic Z, Down JD, Revisiting strain-related differences in radiation sensitivity of the mouse lung: recognizing and avoiding the confounding effects of pleural effusions. Radiat Res 2010; 173, 10–20. [PubMed: 20041755]

27. Jackson IL, Vujaskovic Z, Down JD, A further comparison of pathologies after thoracic irradiation among different mouse strains: finding the best preclinical model for evaluating therapies directed against radiation-induced lung damage. Radiat Res 2011; 175, 510–18. [PubMed: 21338245]

28. Jackson IL, Baye F, Goswami CP, Katz BP, Zodda A, Pavlovic R, et al. , Gene expression profiles among murine strains segregate with distinct differences in the progression of radiation-induced lung disease. Dis Model Mech 2017; 10, 425–37. [PubMed: 28130353]

29. Jackson IL, Zhang Y, Bentzen SM, Hu J, Zhang A, Vujaskovic Z, Pathophysiological mechanisms underlying phenotypic differences in pulmonary radioresponse. Sci Rep 2016; 6, 36579. [PubMed: 27845360]

30. Paun A, Haston CK, Genomic and genome-wide association of susceptibility to radiation-induced fibrotic lung disease in mice. Radiotherapy and oncology : Journal of the European Society for Therapeutic Radiology and Oncology 2012; 105, 350–7. [PubMed: 22954495]

31. Travis EL, Genetic susceptibility to late normal tissue injury. Seminars in Radiation Oncology 2007; 17, 149–55. [PubMed: 17395045]

32. Travis EL, Tucker SL, The relationship between functional assays of radiation response in the lung and target cell depletion. Br J Cancer Suppl 1986; 7, 304–19. [PubMed: 3087402]

33. Colvin GA, Lambert JF, Abedi M, Hsieh CC, Carlson JE, Stewart FM, et al. , Murine marrow cellularity and the concept of stem cell competition: geographic and quantitative determinants in stem cell biology. Leukemia 2004; 18, 575–83. [PubMed: 14749701]

34. MacVittie TJ, Farese AM, Parker GA, Bennett AW, Jackson WE 3rd, Acute Radiation-induced Lung Injury in the Non-human Primate: A Review and Comparison of Mortality and Comorbidities Using Models of Partial-body Irradiation with Marginal Bone Marrow Sparing and Whole Thorax Lung Irradiation. Health Physics 2020; 119, 559–87. [PubMed: 33009295]

35. Van Dyk J, Keane TJ, Kan S, Rider WD, Fryer CJ, Radiation pneumonitis following large single dose irradiation: a re-evaluation based on absolute dose to lung. International Journal of Radiation Oncology, Biology, Physics 1981; 7, 461–7. [PubMed: 7251416]

36. Fish BL, MacVittie TJ, Szabo A, Moulder JE, Medhora M, WAG/RijCmcr rat models for injuries to multiple organs by single high dose ionizing radiation: similarities to nonhuman primates (NHP). Int J Radiat Biol 2020; 96, 81–92. [PubMed: 30575429]

37. Moulder JE, Fish BL, Late toxicity of total body irradiation with bone marrow transplantation in a rat model. International Journal of Radiation Oncology, Biology, Physics 1989; 16, 1501–9.

38. Marx JO, Vudathala D, Murphy L, Rankin S, Hankenson FC, Antibiotic administration in the drinking water of mice. J Am Assoc Lab Anim Sci 2014; 53, 301–6. [PubMed: 24827573]

39. Slate AR, Bandyopadhyay S, Francis KP, Papich MG, Karolewski B, Hod EA, et al. , Efficacy of enrofloxacin in a mouse model of sepsis. J Am Assoc Lab Anim Sci 2014; 53, 381–6. [PubMed: 25199094]

40. Baranov AE, Selidovkin GD, Butturini A, Gale RP, Hematopoietic recovery after 10-Gy acute total body radiation. Blood 1994; 83, 596–9. [PubMed: 8286754]

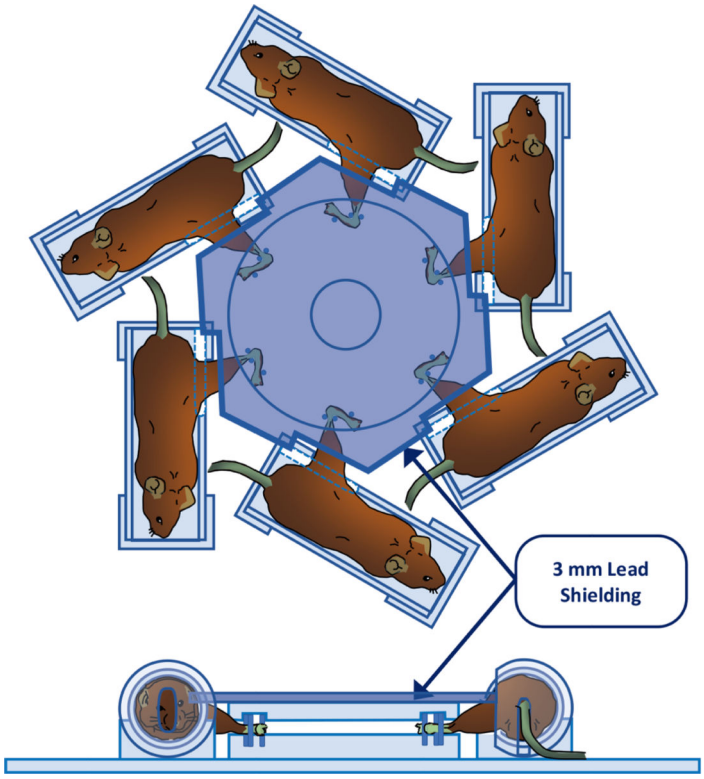

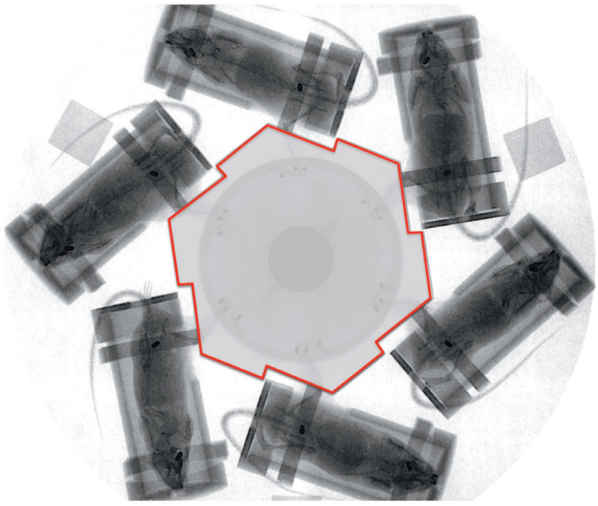

FIG. 1.

Panel A: Schematic illustration of the hexagonal jig and shielding design for uniform total-body irradiation with 2.5% bone marrow sparing. Animals are irradiated in a stationary position using a 320 kV Orthovoltage X-ray radiation source (320 kVp, HVL = 1 mm Cu, dose rate 1.662 ± 0.03 Gy/min, X-Rad 320, Precision X-ray, North Branford, CT). Panel B: Gafchromic film imaging of animals in the irradiation set-up.

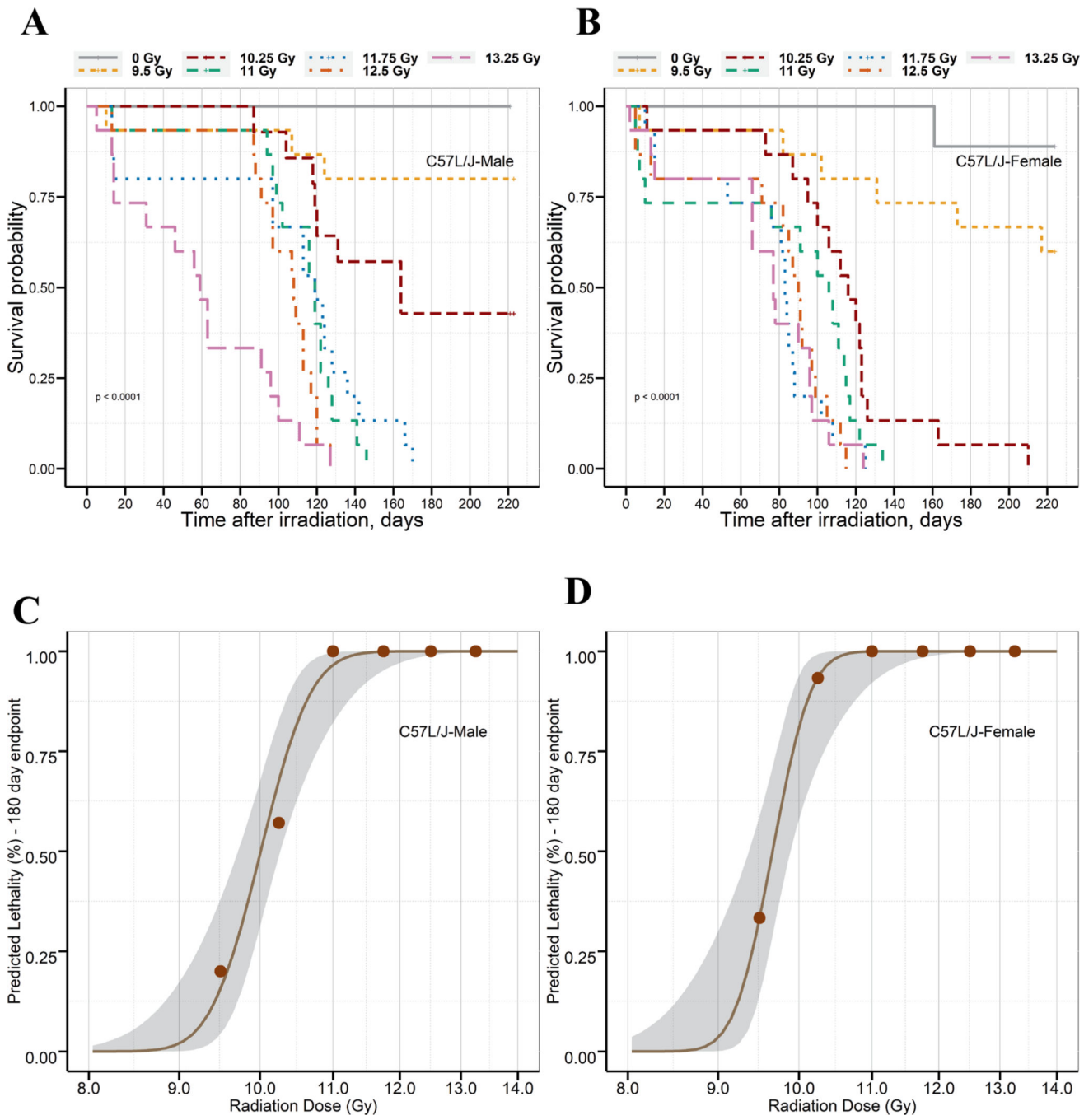

FIG. 2.

Kaplan-Meier curves are presented for 220-day survival in age matched male (panel A) and female (panel B) C57L/J mice exposed to 9.5 to 13.25 Gy TBI/BM2.5, or sham irradiation. The median survival time was estimated as 59–164 days in male mice and 77–116 days in female mice. Probit model predicted lethality of male (panel C) and female (panel D) C57L/J mice (10–12 weeks of age on the day of irradiation) within the first 180 days postirradiation to TBI/BM2.5. The gray region represents the 95% CI of the radiation dose-response curve, and the brown points represent the observed data.

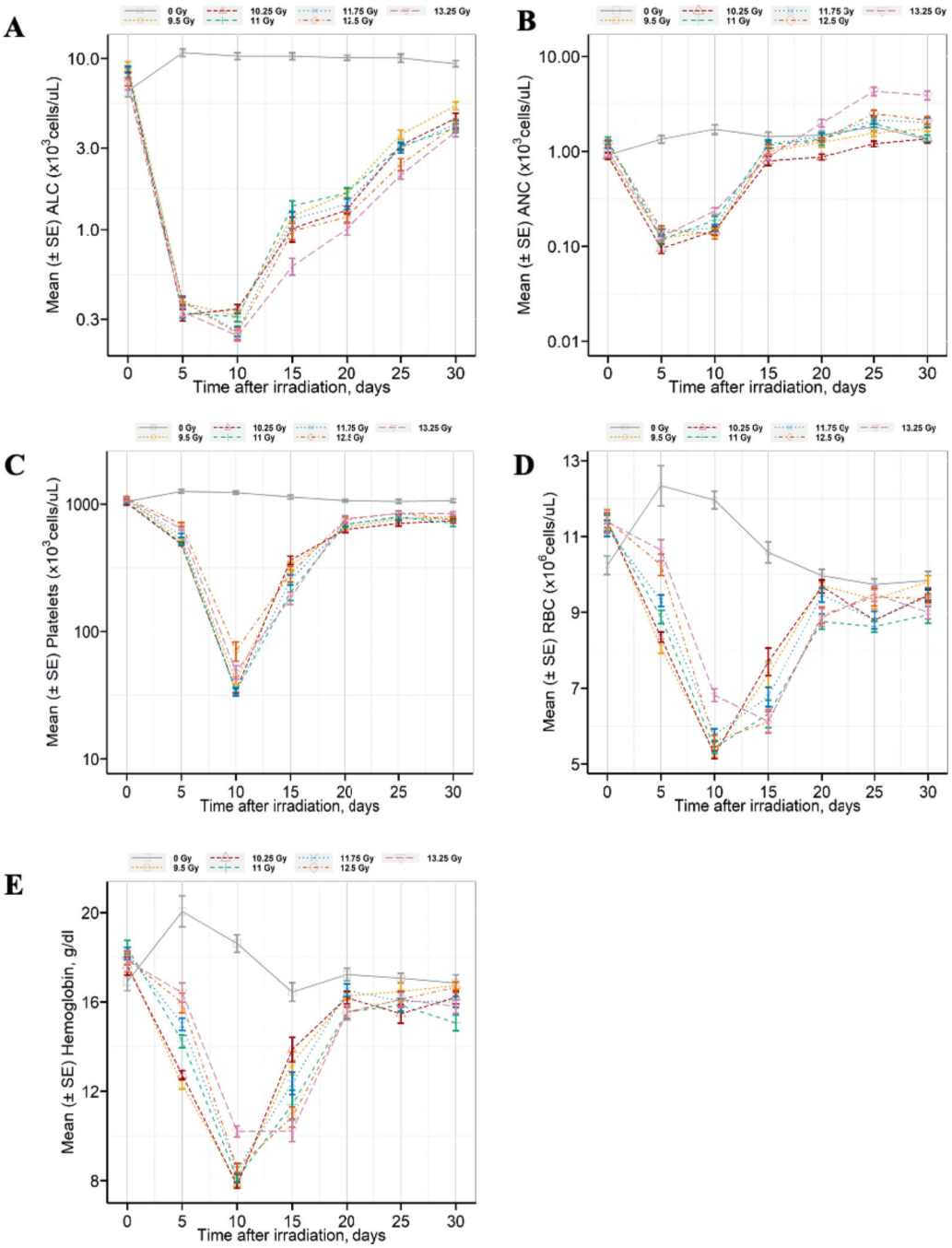

FIG. 3.

Pancytopenia consistent with the hematopoietic subsyndrome of the acute radiation syndrome was observed during the first 30-days postirradiation. Longitudinal changes in panel A absolute lymphocyte count (ALC), panel B) absolute neutrophil count (ANC), panel C) platelet count, panel D) red blood cell (RBC) count, and panel E) hemoglobin during the ARS phase after TBI/BM2.5 in C57L/J mice (n = 14–15 males and 15 females per radiation arm, 10 males and 10 females in the sham-irradiation control arm). Blood was sampled from each animal prior to sham-TBI/BM2.5 or TBI/BM2.5 and on days

5, 10, 15, 20, 25, and 30 postirradiation. Complete blood count with 5-part differential was performed. There was a statistically significant decline in ALC, ANC, RBC, and hemoglobin on day 5 postirradiation ($P = 0.002$). By day 30, the ANC in the 13.25 Gy arm was statistically increased over the sham-irradiation arm ($P < 0.0001$). Hemoglobin levels were not significantly lower than the control arm except in the 11.0 Gy TBI/BM2.5 arm. There was no significant difference in RBC among any radiation arms by day 30. Data are presented as mean ± SE at each time point.

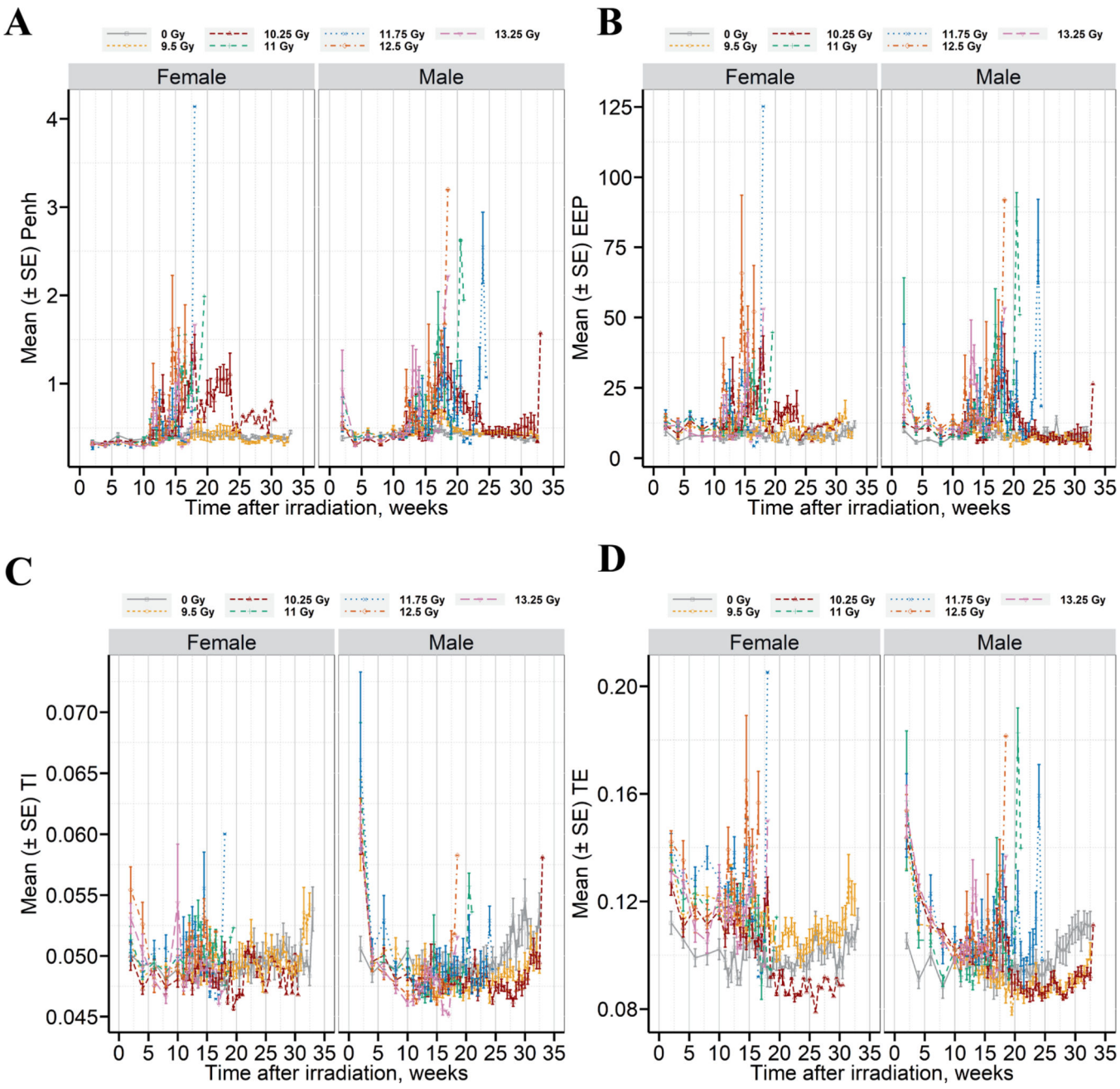

FIG. 4.

Respiratory dysfunction correlates with the temporal onset and progression of radiation pneumonitis/fibrosis. Longitudinal changes are shown for panel A - Penh, panel B -end expiratory pause (EEP), panel C - inspiratory time (TI), panel D - expiratory time (TE). Data are presented as mean ± SE (n = 14–15 male and 15 female per radiation arm, 10 male, 10 female in the sham-control arm), separated by dose and sex.

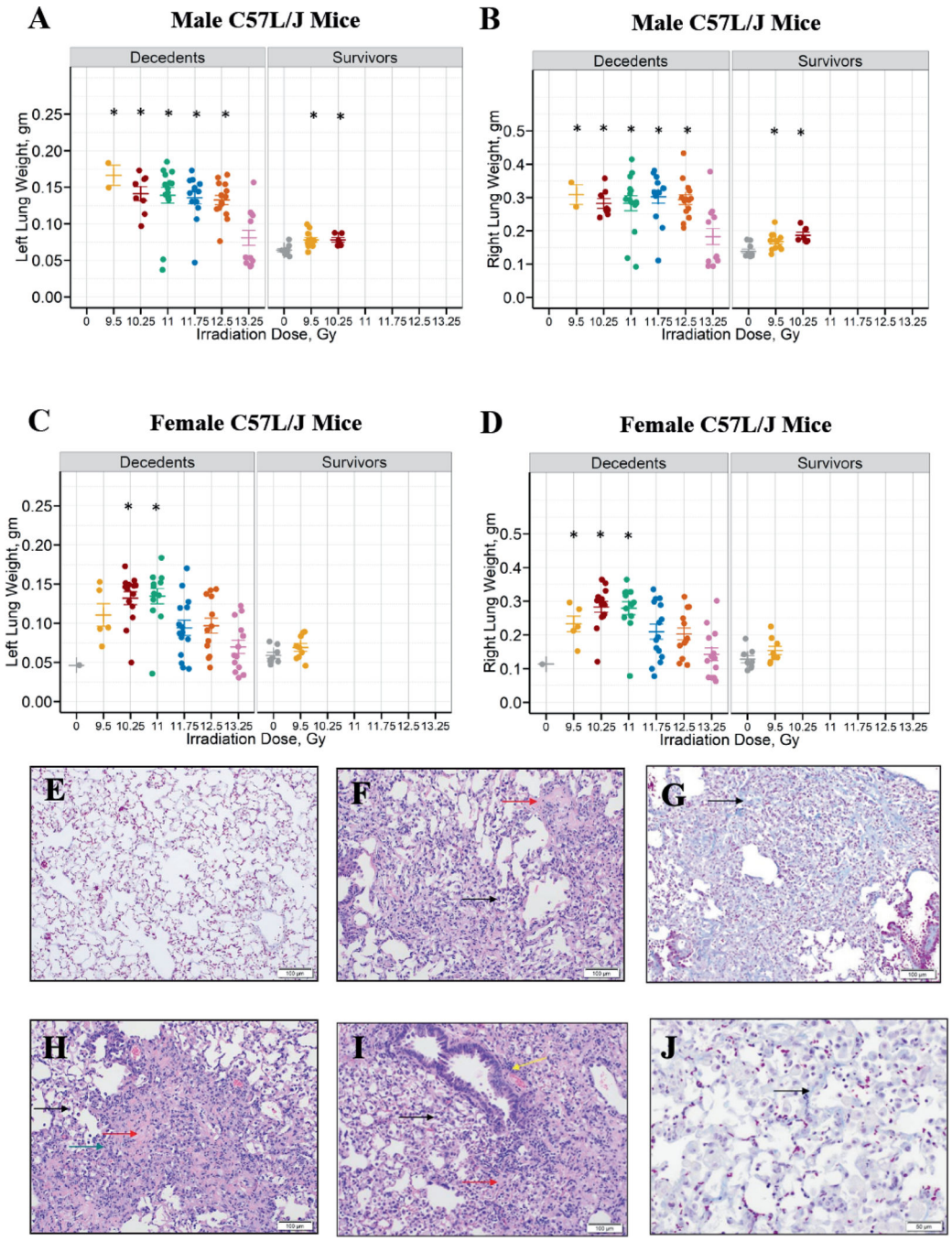

FIG. 5.

Edema/congestion and microscopic abnormalities consistent with radiation pneumonitis and fibrosis in the lungs of C57L/J mice exposed to 9.5–13.25 Gy TBI/BM2.5. Left and right lung weights for male (panels A and B) and female (panels C and D) animals at the time of unscheduled euthanasia (e.g., decedents) or scheduled euthanasia at the study endpoint (e.g., 220-day survivors). The lung weights were compared between sham-irradiated animals and the different radiation groups in males and females, separately, irrespective of survivor status. Kruskal Wallis test at a significance level of 5% was used as a global test. If the

global test was significant, pair-wise comparison adjusting for multiple comparisons by Bonferroni method (adjusted level of significance = 0.0083) was performed. The statistical significance of a radiation group compared to the sham-irradiated group is denoted by an asterisk on the graph. There was a statistically significant difference in wet lung weight between male animals euthanized prior to the 220-day study endpoint and the sham-irradiated controls for all study arms except for 13.25 Gy. In females, left lung weights in the 10.25 and 11 Gy arm and right lung weights in the 9.5, 10.25, and 11 Gy arms were significantly different from the sham-irradiated controls. Panel E: Representative image of normal pulmonary architecture in aged C57L/J mice (i.e., study day 222). Panel F: Mild infiltration of alveolar spaces by macrophages (black arrow) and minimal hyaline membrane formation within the alveoli (red arrow) were a common feature (9.5 Gy, study day 224). Panel G: Moderate interstitial fibrosis (black arrow) with thickening of alveolar septa and occasional nodular thickening (modified ashcroft score = 5) were observed (9.5 Gy, study day 224). Panel H: Moderate infiltration of alveolar spaces by macrophages (black arrow), mild hyaline membrane formation (red arrow), and mild mixed cell inflammation of the interstitium (green arrow) (10.25 Gy, study day 121). Panel I: There was moderate infiltration of alveolar spaces by macrophages (black arrow), moderate hyaline membrane formation within alveoli (red arrow), and mild perivascular infiltration by mononuclear cells (yellow arrow) in the lungs on day 112 after 13.25 Gy. Panel J: There was mild interstitial fibrosis (arrow) with thickening of alveolar septa (modified ashcroft score = 3) on day 128 after 13.25 Gy. All photomicrographs are 10× magnification, unless otherwise noted.

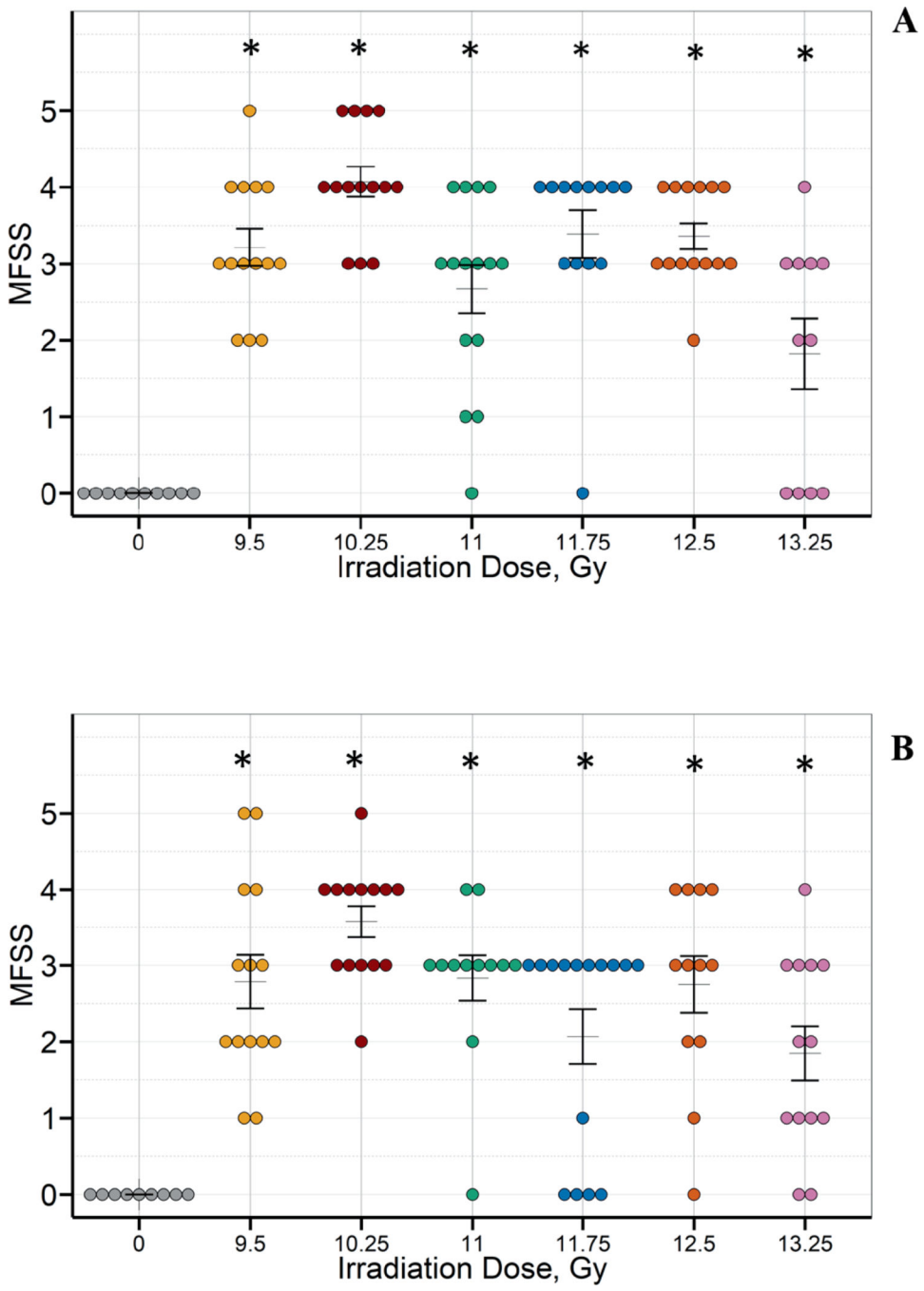

FIG. 6.

There was a significant increase in lung fibrosis among irradiated male (panel A) and female (panel B) C57L/J mice in all study arms compared to the sham-irradiated controls. The MFSS scores were compared between sham-irradiated animals and the different radiation groups in males and females separately irrespective of survivor status. Kruskal Wallis test at a significance level of 5% was used as a global test. If the global test was significant, pair-wise comparison adjusting for multiple comparisons by Bonferroni method (adjusted level of significance = 0.0083) was performed. The statistical significance of a radiation group

compared to the sham-irradiated group is denoted by an asterisk on the graph. Masson's trichrome stained lung sections were scored by a board-certified veterinary pathologist using a modified fibrosis scoring system (MFSS). (Hübner RH, Gitter W, El Mokhtari NE, Mathiak M, Both M, Bolte H, Freitag-Wolf S, B Bewig. Standardized quantification of pulmonary fibrosis in histological samples. BioTechniques 44:507–517, 2008.)

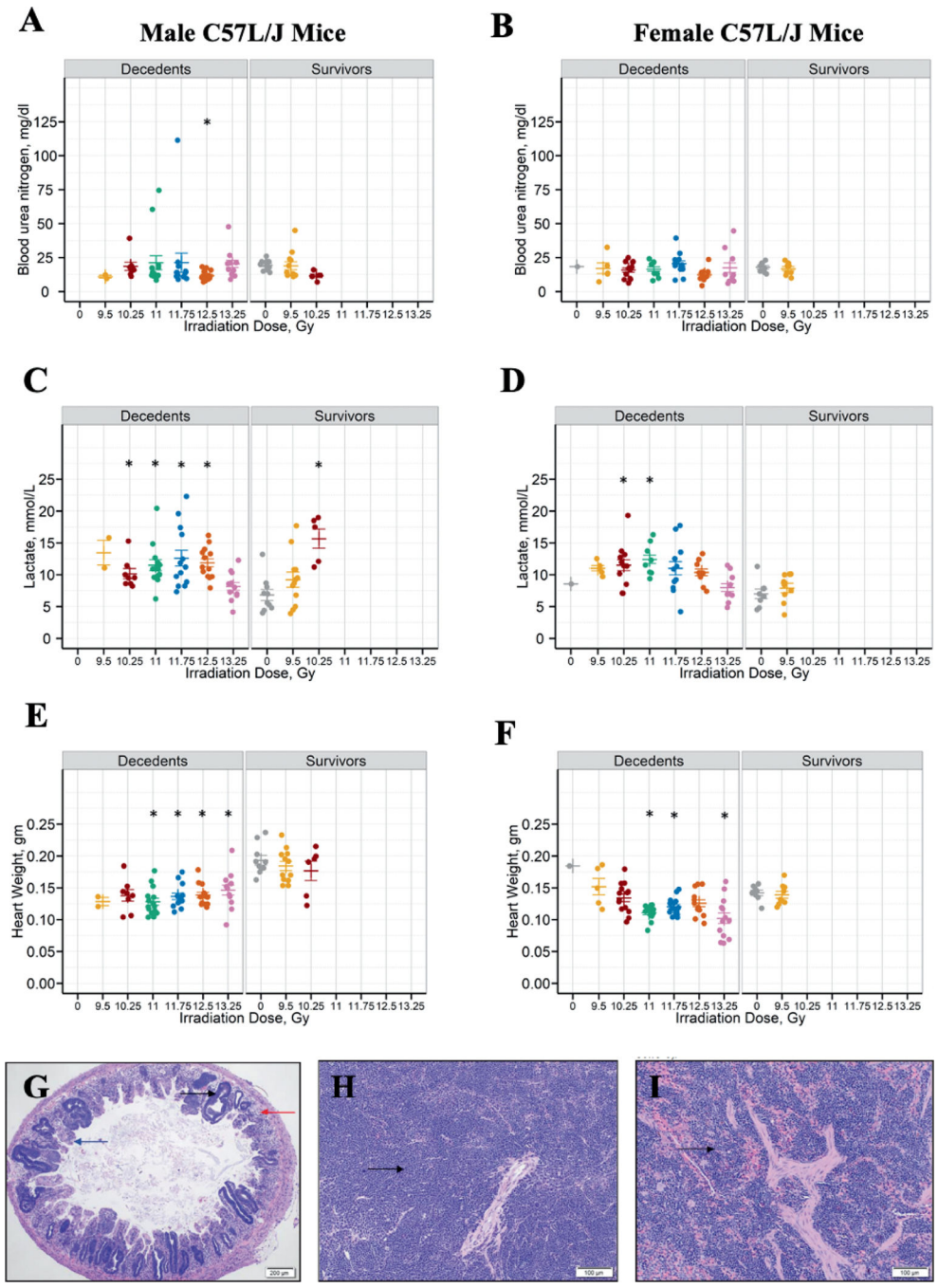

FIG. 7.

Multiorgan injury after TBI/BM2.5. Blood urea nitrogen (BUN) levels in male and female C57L/J mice at the time of unscheduled euthanasia (e.g., decedents) or scheduled euthanasia after the 220-day study endpoint (panel A: male; panel B: female). BUN, lactate levels and heart weight were compared between sham-irradiated animals and the different radiation groups in males and females separately irrespective of survivor status. Kruskal Wallis test at a significance level of 5% was used as a global test. If the global test was significant, pair-wise comparison adjusting for multiple comparisons by Bonferroni method (adjusted

level of significance = 0.0083) was performed. The statistical significance of a radiation group compared to the sham-irradiated group is denoted by an asterisk on the graph. Blood lactate levels (panel C: male; panel D: female) were significantly elevated among male C57L/J 220-day survivors in the 10.25 Gy arm compared to the sham-irradiated controls. Elevation in blood lactate levels suggests impairment in tissue oxygenation. Heart weight was significantly decreased among animals euthanized prior to the study endpoint due to criteria across all radiation arms (panel E: male; Panel F: female). Panel G: The Jejunum of a mouse on day 6 after 13.25 Gy TBI/BM2.5 shows marked crypt hyperplasia (black arrow), severe villus blunting (blue arrow) and moderate degeneration (red arrow) and loss of crypts. 4× magnification. Panel H: Severe lymphoid depletion and severely increased extramedullary hematopoiesis (black arrow) was observed in the spleen on day 14 after 11 Gy TBI/BM2.5. Panel I: Extramedullary hematopoiesis (black arrow) of the spleen was markedly increased on study day 132 after 10.25 Gy TBI/BM2.5. All images are 10× magnification unless otherwise noted.

TABLE 1

Median Survival Time (95% CI) in C57L/J Mice after TBI/BM2.5 in the Dose Range of 9.5 to 13.25 Gy

Radiation group	Median survival time, days (95% CI)		
	Male	Female	Mixed sex
Sham (0 Gy)	NA	NA	NA
9.5 Gy	NA	NA	NA
10.25 Gy	164 (120, NA)	116 (100,126)	122 (118,164)
11 Gy	119 (102,128)	106 (76,117)	112.5 (100,119)
11.75 Gy	119 (97,142)	83 (76,102)	92.5 (83,119)
12.5 Gy	108 (97,120)	90 (82,105)	97 (90,109)
13.25 Gy	59 (31,100)	77 (66,97)	66.0 (59,96)

TABLE 2

Lethal Dose (LD)10–99/180 in C57L/J Mice Exposed to TBI/BM2.5

Percent lethality	Males		Females		Mixed sex	
	Lethal dose	95% CI	Lethal dose	95% CI	Lethal dose	95% CI
10	9.37	8.99, 9.76	9.19	8.83, 9.56	9.22	8.93, 9.52
20	9.58	9.27, 9.91	9.35	9.06, 9.65	9.42	9.19, 9.67
30	9.74	9.46, 10.03	9.47	9.22, 9.72	9.58	9.37, 9.78
40	9.88	9.63, 10.14	9.57	9.34, 9.79	9.71	9.52, 9.89
50	10.01	9.77, 10.26	9.66	9.45, 9.87	9.83	9.66, 10.00
60	10.14	9.90, 10.39	9.76	9.55, 9.97	9.96	9.79, 10.13
70	10.29	10.02, 10.55	9.86	9.64, 10.09	10.09	9.91, 10.13
80	10.46	10.15, 10.77	9.98	9.73, 10.25	10.25	10.05, 10.47
90	10.70	10.32, 11.09	10.16	9.83, 10.50	10.48	10.22, 10.76
99	11.29	10.66, 11.96	10.58	10.03, 11.16	11.05	10.60, 11.52

Radiat Res. Author manuscript; available in PMC 2024 April 01.

TABLE 3

Neutrophil Related Parameters in Male and Female C57L/J Mice after TBI/BM2.5

Radiation dose (Gy)	C57L/J mice		Time (days) to first day ANC < 100 cells/μL or 500 cells/μL		Duration (days) of ANC < 100 cells/μL or 500 cells μL		Recovery (days) of ANC >1,000 cells/μL	ANC Nadir × 100 cells/μL
			<100 cells/μL	<500 cells/μL	<100 cells/μL	<500 cells/μL		
9. 5 Gy	Male (n = 15)	Mean ± SD	7.5 ± 2.5	6.0 ± 2.0	1.2 ± 2.5	4.7 ± 3.5	14.5 ± 4.7	0.188 ± 0.166
		Median	7.5	5	0	5	15	0.120
		Range	(5, 10)	(5, 10)	(0, 5)	(0, 10)	(5, 20)	(0.072, 0.735)
	Female (n = 15)	Mean ± SD	5.9 ± 1.9	5.3 ± 1.2	1.4 ± 2.3	4.7 ± 2.3	12.9 ± 5.4	0.137 ± 0.077
		Median	5	5	0	5	10	0.136
		Range	(5, 10)	(5, 10)	(0, 5)	(0,10)	(5, 25)	(0.020, 0.312)
	Overall (n = 30)	Mean ± SD	6.3 ± 2.3	6.1 ± 2.1	1.3 ± 2.3	4.7 ± 2.9	13.7 ± 5.1	0.164 ± 0.131
		Median	5	5	0	5	15	0.128
		Range	(5, 10)	(5, 15)	(0, 5)	(0,10)	(5, 25)	(0.020, 0.735)
10.25 Gy	Male (n = 14)	Mean ± SD	6.9 ± 2.4	7.7 ± 3.2	0.6 ± 1.8	4.3 ± 5.8	12.3 ± 5.6	0.293 ± 0.263
		Median	5	5	0	2.5	10	0.200
		Range	(5, 15)	(5, 15)	(0, 5)	(0, 20)	(5, 20)	(0.048, 0.837)
	Female (n = 15)	Mean ± SD	6.2 ± 2.2	6.3 ± 2.2	1.9 ± 2.6	6.7 ± 4.9	12.9 ± 5.4	0.187 ± 0.175
		Median	5	5	0	5	25	0.140
		Range	(5, 10)	(5, 10)	(0, 5)	(0, 15)	(5, 25)	(0.048, 0.741)
	Overall (n = 29)	Mean ± SD	6.6 ± 2.4	7.0 ± 2.8	1.2 ± 2.2	5.5 ± 5.4	12.6 ± 5.4	0.238 ± 0.224
		Median	5	5	0	5	15	0.168
		Range	(5, 10)	(5, 15)	(0, 5)	(0, 20)	(5, 25)	(0.048, 0.837)
11 Gy	Male (n = 15)	Mean ± SD	5.0 ± 0.0	6.1 ± 2.1	0 ± 0	3.9 ± 2.1	10.4 ± 4.5	0.253 ± 0.133
		Median	5	5	0	5	10	0.216
		Range	(5, 10)	(5, 10)	(0, 0)	(0, 5)	(5, 15)	(0.011, 0.555)
	Female (n = 15)	Mean ± SD	5.6 ± 1.6	5.8 ± 1.8	1.1 ± 2.2	8.5 ± 9.0	10.4 ± 3.6	0.138 ± 0.057
		Median	5	5	0	5	10	0.124
		Range	(5, 10)	(5, 10)	(0, 5)	(0, 30)	(5, 15)	(0.070, 0.240)
	Overall (n = 30)	Mean ± SD	5.4 ± 1.4	5.9 ± 2.0	0.8 ± 2.0	6.1 ± 6.7	10.4 ± 4.0	0.202 ± 0.120
		Median	5	5	0	5	10	0.168

Radiation dose (Gy)	C57L/J mice		Time (days) to first day ANC < 100 cells/μL or 500 cells/μL		Duration (days) of ANC < 100 cells/μL or 500 cells μL		Recovery (days) of ANC >1,000 cells/μL	ANC Nadir × 100 cells/μL
			<100 cells/μL	<500 cells/μL	<100 cells/μL	<500 cells/μL		
		Range	(5, 10)	(5, 10)	(0, 5)	(0, 30)	(515)	(0.070, 0.555)
11.75 Gy	Male (n = 15)	Mean ± SD	7.1 ± 2.5	5.3 ± 1.2	0 ± 0	4.0 ± 2.1	13.8 ± 3.1	0.216 ± 0.128
		Median	5	5	0	5	15	0.192
		Range	(5, 10)	(5, 10)	(0, 0)	(0, 5)	(10, 20)	(0.064, 0.570)
	Female (n = 15)	Mean ± SD	6.4 ± 2.3	6.1 ± 2.1	1.4 ± 2.4	4.6 ± 5.0	12.1 ± 4.5	0.206 ± 0.209
		Median	5	5	0	5	12.5	0.144
		Range	(5, 10)	(5, 10)	(0, 5)	(0, 20)	(5, 20)	(0.048, 0.756)
	Overall (n = 30)	Mean ± SD	6.8 ± 2.5	5.7 ± 1.8	0.7 ± 1.8	4.3 ± 3.7	12.9 ± 3.9	0.211 ± 0.173
		Median	5	5	0	5	15	0.164
		Range	(5, 10)	(5, 10)	(0, 5)	(0, 20)	(5, 20)	(0.048, 0.756)
12.5 Gy	Male (n = 15)	Mean ± SD	8.0 ± 2.5	5.7 ± 1.7	1.0 ± 2.1	4.3 ± 2.7	14.2 ± 4.2	0.266 ± 0.472
		Median	10	5	0	5	15	0.096
		Range	(5, 10)	(5, 10)	(0, 5)	(0, 10)	(5, 20)	(0.030, 1.653)
	Female (n = 15)	Mean ± SD	5.0 ± 0.0	5.8 ± 1.9	1.7 ± 2.9	3.8 ± 2.3	13.2 ± 8.2	0.252 ± 0.186
		Median	5	5	0	5	12.5	0.192
		Range	(5, 5)	(5, 10)	(0, 5)	(0, 5)	(5, 30)	(0.036, 0.690)
	Overall (n = 30)	Mean ± SD	7.3 ± 2.6	5.8 ± 1.8	1.2 ± 2.2	4.0 ± 2.5	13.6 ± 6.6	0.259 ± 0.362
		Median	5	5	0	5	15	0.132
		Range	(5, 10)	(5, 10)	(0, 5)	(0, 10)	(5, 30)	(0.03, 1.653)
13.25 Gy	Male (n = 15)	Mean ± SD	8.0 ± 4.0	7.5 ± 2.5	0 ± 0	3.2 ± 3.2	10.4 ± 5.2	0.588 ± 1.401
		Median	7.5	7.5	0	5	10	0.216
		Range	(5, 15)	(5, 10)	(0, 0)	(0, 10)	(5, 20)	(0.080, 5.445)
	Female (n = 15)	Mean ± SD	6.7 ± 2.4	5.7 ± 1.8	0.8 ± 2.0	5.7 ± 2.7	10.9 ± 4.4	0.296 ± 0.240
		Median	5	5	0	5	10	0.288
		Range	(5, 10)	(5, 10)	(0, 4)	(0, 10)	(5, 15)	(0.064, 1.064)
	Overall (n = 30)	Mean ± SD	7.3 ± 3.4	6.6 ± 2.4	0.4 ± 1.5	4.5 ± 3.1	10.6 ± 4.7	0.437 ± 0.981
		Median	5	5	0	5	10	0.260
		Range	(5, 15)	(5, 10)	(0, 5)	(0, 10)	(5, 20)	(0.064, 5.445)

TABLE 4

Statistical Comparisons of Lung Weight after Sham Irradiation or TBI/BM2.5 in Males and Female Mice

	Males	Females
Left lung weight[a]	**9.5 Gy vs. Sham: P = 0.0014**	9.5 Gy vs. Sham: P = 0.0181
	10.25 Gy vs. Sham: P = 0.0001	**10.25 Gy vs. Sham: P = 0.0004**
	11 Gy vs. Sham: P = 0.0025	**11 Gy vs. Sham: P = 0.0015**
	11.75 Gy vs. Sham: P = 0.0007	11.75 Gy vs. Sham: P = 0.0204
	12.5 Gy vs. Sham: P < 0.0001	12.5 Gy vs. Sham: P = 0.0104
	13.25 Gy vs. Sham: P = 0.7513	13.25 Gy vs. Sham: P = 0.6402
Right lung weight[a]	**9.5 Gy vs. Sham: P = 0.0054**	**9.5 Gy vs. Sham: P = 0.0074**
	10.25 Gy vs. Sham: P = 0.0001	**10.25 Gy vs. Sham: P = 0.0001**
	11 Gy vs. Sham: P = 0.0025	**11 Gy vs. Sham: P = 0.0015**
	11.75 Gy vs. Sham: P = 0.0007	11.75 Gy vs. Sham: P = 0.0170
	12.5 Gy vs. Sham: P < 0.0001	12.5 Gy vs. Sham: P = 0.0094
	13.25 Gy vs. Sham: P = 0.8053	13.25 Gy vs. Sham: P = 0.7894

[a]Bonferroni adjusted level of significance = 0.0083.

Notes. Any P value less than 0.008 is statistically significant. Significant values are in bold.

TABLE 5

Statistical Comparisons between Treatment Arms for Blood Urea Nitrogen, Lactate Levels and Heart Weights

	Males	Females
BUN[a]	9.5 Gy vs. Sham: P = 0.1198	Global test not significant
	10.25 Gy vs. Sham: P = 0.0214	
	11 Gy vs. Sham: P = 0.0258	
	11.75 Gy vs. Sham: P= 0.0108	
	12.5 Gy vs. Sham: P =0.0007	
	13.25 Gy vs. Sham: P = 0.6982	
Lactate[a]	9.5 Gy vs. Sham: P = 0.0693	9.5 Gy vs. Sham: P = 0.0725
	10.25 Gy vs. Sham: P = 0.0011	**10.25 Gy vs. Sham: P = 0.0025**
	11 Gy vs. Sham: P = 0.0021	**11 Gy vs. Sham: P = 0.0017**
	11.75 Gy vs. Sham: P= 0.0014	11.75 Gy vs. Sham: P= 0.0185
	12.5 Gy vs. Sham: P = 0.0007	12.5 Gy vs. Sham: P = 0.0107
	13.25 Gy vs. Sham: P = 0.1927	13.25 Gy vs. Sham: P = 0.4799
Heart weight[a]	9.5 Gy vs. Sham: P = 0.2299	9.5 Gy vs. Sham: P = 0.5495
	10.25 Gy vs. Sham: P = 0.0281	10.25 Gy vs. Sham: P = 0.2439
	11 Gy vs. Sham: P < 0.0001	**11 Gy vs. Sham: P = 0.0003**
	11.75 Gy vs. Sham: P= 0.0001	**11.75 Gy vs. Sham: P= 0.0015**
	12.5 Gy vs. Sham: P < 0.0001	12.5 Gy vs. Sham: P = 0.0506
	13.25 Gy vs. Sham: P = 0.0013	**13.25 Gy vs. Sham: P = 0.0045**

[a]Bonferroni adjusted level of significance = 0.0083.

Notes. Any P value less than 0.008 is statistically significant. Significant values are in bold.